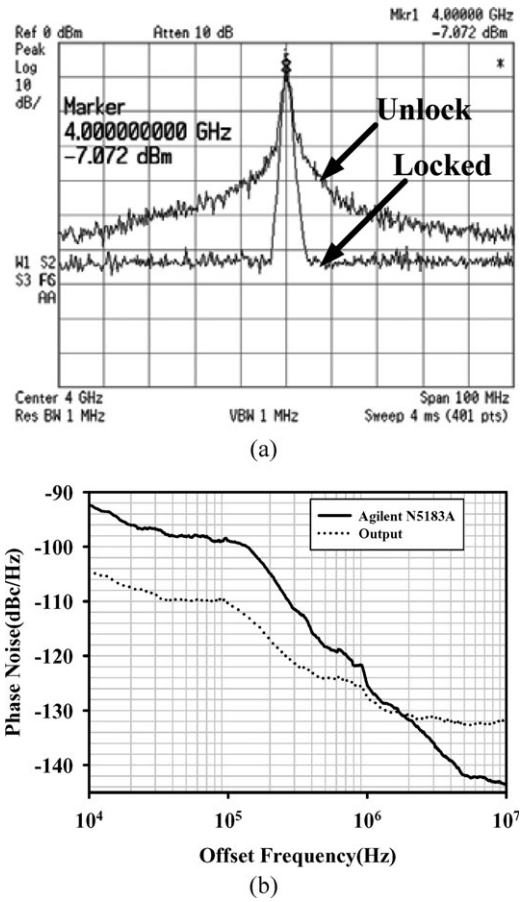

Figure 5 (a) Measured locked and free-running spectra of the divide-by-4 ILFD. (b) Measured phase noises of the injection-reference and the locked divide-by-4 ILFD. $V_{DD} = 1.5$ V, $V_{bias} = 2.05$ V, $V_{inj} = 1$ V, injection signal = 16 GHz, and divider output = 4 GHz

TABLE 1 Performance Comparison of BiCMOS ILFDs

Ref.	Tech (um)	Mod.	Pin (dBm)	*V*DD (V)/ Pdis (mW)	Locking Range
[1]	0.35	÷4	0	3.1/6.6	8.7–8.86 (1.82)
[3]	0.18	÷4	0	3.6/50.4	59.77–60.12 (0.6)
[5]	0.18	÷3	–	2.5/15	75.67–78.5 (3.67)
[6]	0.35	÷4	0	3/4.32	14.6–15 (2.7)
This	0.18	÷4	0	1.5/1.5	14.6–16.3 (11)

4. CONCLUSION

A low power, wide locking range divide-by-4 injection locked frequency divider has been proposed and fabricated in TSMC 0.18 μm SiGe BiCMOS technology. The proposed divide-by-4 ILFD uses the cross-coupled HBT VCO as the core to have a low power and a two-nMOSFETs and one-pMOSFET composite to emulate a linear injection mixer, so that a wider locking range divide-by-4 ILFD can be designed. Increasing the strength of the second harmonic signal at the tail inductor is an essential approach to enhance locking range. At the supply voltage of 1.5 V and at the incident power of 0 dBm, the locking range of the divide-by-4 is 1.4 GHz, from the incident frequency 14.6 to 16.3 GHz, the percentage is 11%.

ACKNOWLEDGMENT

The authors would like to thank the Staff of the CIC for the chip fabrication and technical supports.

REFERENCES

1. S.-L. Jang, C.C. Liu, and C.-W. Chung, A tail-injected divide-by-4 SiGe HBT injection locked frequency divider, IEEE Microwave Wireless Compon Lett 19 (2009), 236–238.
2. S. Trotta et al., A new regenerative divider by four up to 160 GHz in SiGe bipolar technology, In Proceedings of IEEE International Microwave Symposium, San Francisco, CA, 2006, pp. 1709–1712.
3. J.-C. Chien, C.-S. Lin, L.-H. Lu, H. Wang, J. Yeh, C.-Y. Lee, and J. Chern, A harmonic injection-locked frequency divider in 0.18-μm SiGe BiCMOS, IEEE Microwave Wireless Compon Lett 16 (2006), 561–563.
4. K. Yamamoto and M. Fujishima, 70 GHz CMOS harmonic injection locked divider, In: IEEE International Solid-State Circuits Conference Digest, San Francisco, CA, February 2006, pp. 2472–2481.
5. V. Jain, B. Javid, and P. Heydari, A BiCMOS dual-band millimeter-wave frequency synthesizer for automotive radars, IEEE J Solid-State Circuits 44 (2009), 2100–2113.
6. S.-L. Jang, C.-W. Chang, C.-L. Cheng, C.-W. Hsue, and C.-W. Hsu, A wide-locking range SiGe BiCMOS divide-by-3 injection-locked oscillators, IEEE International Symposium on VLSI Design, Automation and Test (VLSI-DAT), 2011, pp. 1–4.

LEFT-HANDED METAMATERIAL STRUCTURE INCORPORATED WITH MICROSTRIP ANTENNA

M. K. A. Rahim, N. Ibrahim, H. A. Majid, and N. A Murad
Radio Communication Engineering Department (RaCED), Universiti Teknologi Malaysia (UTM), 81310 UTM JB, Johor, Malaysia; Corresponding author: mkamal@fke.utm.my

Received 7 March 2012

ABSTRACT: *This article presents the design, simulation, and fabrication of a new planar left-handed metamaterial (LHM), which consist of a combination of a modified square rectangular split ring resonator and strip wire. Both structures are on the same plane. The structure is simulated and measured with the microstrip antenna operating at frequency 5.8 GHz. The LHM has been analyzed using Nicolson–Ross–Weir approach to obtain the negative permeability and permittivity at 5.8 GHz. The fabrication of the LHM is on FR-4 board substrate. From the simulation and measurement results, the gain of the microstrip antenna with LHM has increased by 4.0 dB. The return loss of the antenna with LHM is improved to 15.7 dB compare without LHM structure.* © 2012 Wiley Periodicals, Inc. Microwave Opt Technol Lett 54:2828–2832, 2012; View this article online at wileyonlinelibrary.com. DOI 10.1002/mop.27186

Key words: *left handed; gain enhancement; negative permeability; negative permittivity; metamaterial*

1. INTRODUCTION

Left-handed metamaterial (LHM) is a material with simultaneously negative values of dielectric permittivity (ε) and magnetic permeability (μ). In 1968, Veselago [1] studied LHM concept and he made a theoretical speculation of this material that exhibit negative permittivity and permeability. In this medium, the electric field, the magnetic field, and the propagation vector k form a left-handed triad. This medium is called LHM due to this relationship. Recently, metamaterials with simultaneously negative values of dielectric permittivity and magnetic permeability have been discussed in many articles [2–5]. An array of strip wires (SW) has shown to have plasma frequency in the microwave regime. When lower than the plasma frequency, this

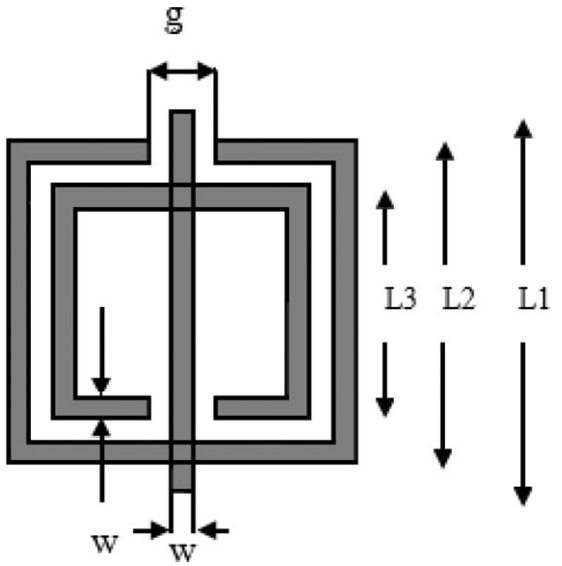

Figure 1 Front view of LHM

structure can produce an effective negative permittivity [6]. An array composed of split ring resonators (SRR) is proposed that exhibited a negative magnetic permeability in the resonance region [7]. The first double negative medium is proposed when these two structures are combined, and it is shown that the electric permittivity and the magnetic permeability are negative [8]. Double negative metamaterials are widely used in the field of antenna to effectively enhance the directivity and the gain of antenna [9–12]. This article discusses the characteristics of the microstrip antenna with and without the LHM structure. The LHM structure's design consists of a combination of a modified SRR and SW, where both structures are on the same plane. The LHM and the microstrip antenna are designed to operate at 5.8 GHz. The negative permittivity and negative permeability of the simulated LHM structures are presented. Both LHM and the antenna have been investigated to operate at 5.8 GHz.

1.1. LHM Design

Figure 1 illustrates the LHM structure where it is a combination of a modified square rectangular SRR and SW. The combination structure is designed on a single plane. The modified SRR will produce magnetic material-like responses and exhibit the negative permittivity and the SW will produce strong dielectric-like responses and exhibit the negative permeability [13]. The dimensions of the structure are shown in Figure 1. The structure

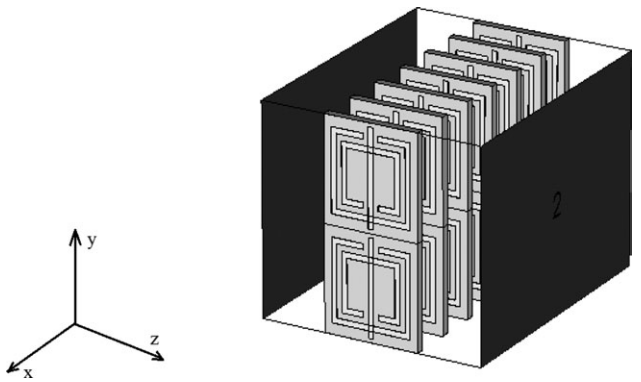

Figure 2 LHM structure in CST environment

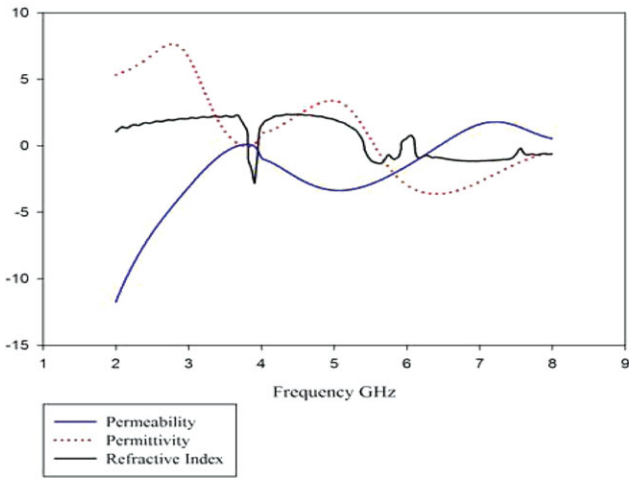

Figure 3 The effective parameter for different frequencies. [Color figure can be viewed in the online issue, which is available at wileyonlinelibrary.com]

consists of one SRR and one SW in the middle of SRR in planar form. The optimized frequency at 5.8 GHz for all dimensions is shown in Figure 1. The gap between SRR, g is 3 mm, the width of SRR and SW w is 1 mm. The height of the strip, t is 0.035 mm and the length of strip is $L_1 = 17.16$ mm, the length of the outer SRR, L_2 is 13.676 mm, and the inner SRR is $L_3 = 10.556$ mm. The dielectric constant of the substrate is 4.5 with a thickness of 1.6 mm and a tangential loss of 0.019.

The simulation of the LHM structure is executed using Computer Simulation Technology (CST) software. Figure 2 shows the array of (2 × 7) cell of the LHM simulated using the CST software. The environment is set to be perfect magnetic conductor on the front and back faces of the block and perfect electric conductor on the top and bottom of the block. The E-field of the incident wave is polarized along y-axis, whereas the H-field of the incident wave is polarized along z-axis.

After extracting the S-parameters data from the simulation, the data are exported to MathCAD. The effective values of permittivity and permeability are calculated by using Nicolson–

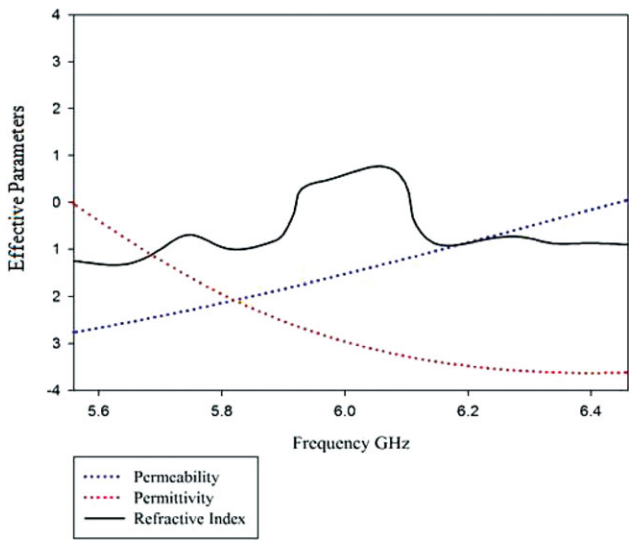

Figure 4 Zoomed in graph of the negative parameters. [Color figure can be viewed in the online issue, which is available at wileyonlinelibrary.com]

TABLE 1 Rectangular Patch Microstrip Antenna Specifications

Parameter	Magnitude	Unit
Operating frequency	5.8	GHz
Length (L)	10.897	mm
Width (W)	14.6	mm
Feed	Coaxial	–
Feed location	$X = 0, Y = -3$	mm

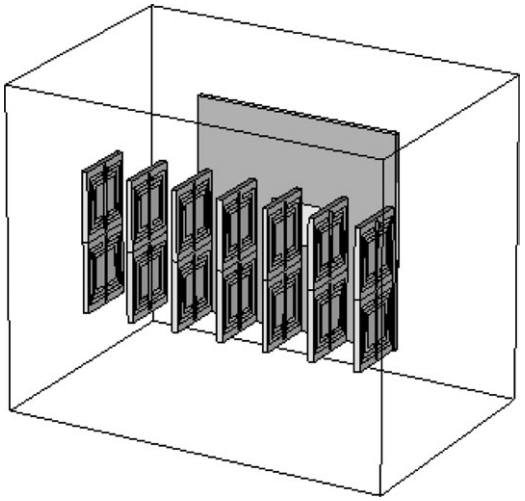

Figure 5 Perspective view of the integration of LHM and microstrip antenna

Ross–Weir approach [5] and the results obtained are shown in Figures 3 and 4.

Referring to Figure 3, the range of the negative permittivity and negative permeability ($-\varepsilon_r$ and $-\mu_r$) starts from 5.6 to 5.95 GHz. The refractive index at 5.8 GHz is -0.95.

1.2. LHM with Antenna

Microstrip antenna is designed to operate at frequency range where both values of permittivity and permeability are negative. In this article, the frequency of 5.8 GHz is chosen for the microstrip antenna's operating frequency and the antenna's specifications are shown in Table 1. In addition, the same material of LHM is used for the microstrip antenna and the LHM structure

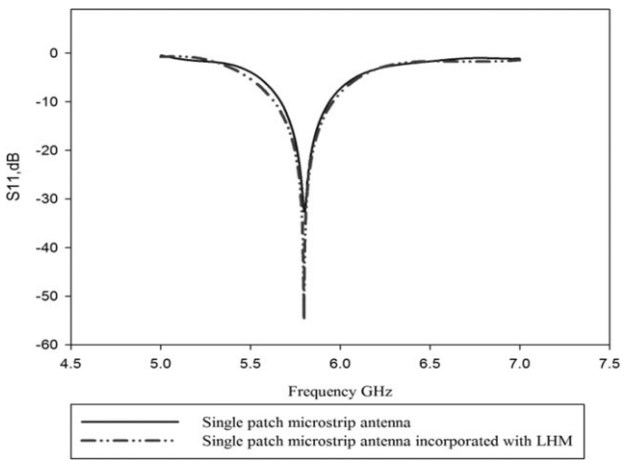

Figure 6 Return loss, S_{11}

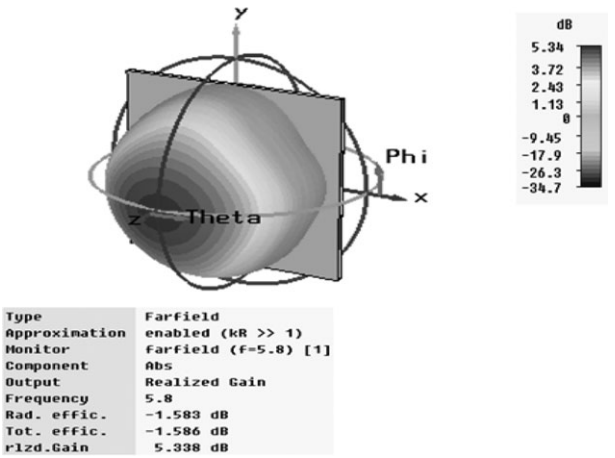

Figure 7 Radiation pattern of single patch microstrip antenna

is placed in front of the microstrip antenna with a distance of 22.5 mm from the ground plane and the gap between the slabs is 13.6 mm as shown in Figure 5.

2. RESULT AND DISCUSSION

The simulated return loss is shown in Figure 6. It shows a good agreement between microstrip antenna with and without LHM where both resonate at 5.8 GHz. Figures 7 and 8 shows the simulated three-dimensional radiation pattern of microstrip

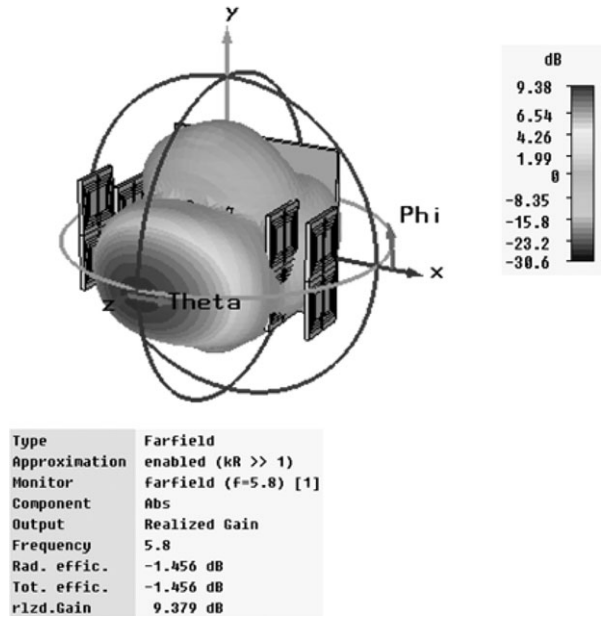

Figure 8 Radiation pattern of single patch microstrip antenna integrated with LHM structure

TABLE 2 Comparison of Simulation Result

	Parameters	Without LH MTM (5.8 GHz)	With LH MTM (5.8 GHz)
1	Return loss (S_{11})	−32.7 dB	−48.41 dB
2	Gain	5.34 dB	9.38 dB
3	Directivity	6.92 dBi	10.8 dBi
4	HPBW	85.5°	51.1°

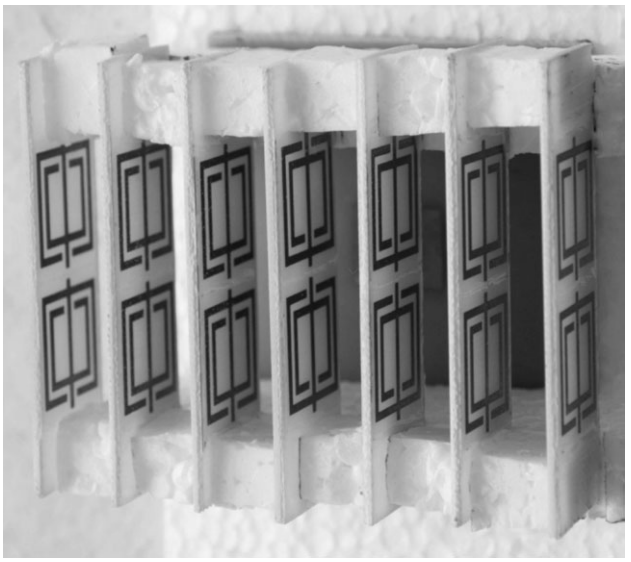

Figure 9 Fabrication of LHM with square patch antenna

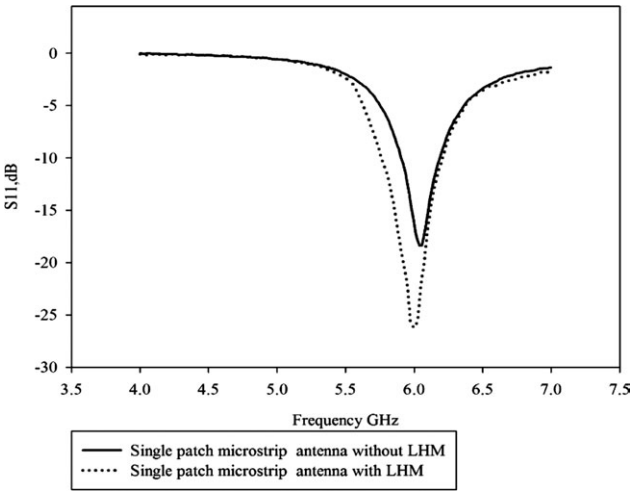

Figure 10 Measured S_{11} of the microstrip antenna with and without LHM

antenna with and without LHM. Comparison between gain/directivity of both radiation patterns shows an increasing of gain/directivity up to 4.0 dB only by attaching the LHM in front of the microstrip antenna. To illustrate the difference between the response of the microstrip antenna in the presence of the LHM or not, Table 2 has been constructed. In that particular table, it is obvious that the S_{11}, gain, and directivity had produced encouraging results for further fabrication processes.

The structure is fabricated on FR-4 Board as shown in Figure 9. Then, the measurement of the S_{11} of the patch antenna with and without LHM is done with the assistance of the vector network analyzer, anechoic chamber, spectrum analyzer, and signal generator. The return loss result is obtained as shown in Figure 10. It shows that the bandwidth of the antenna has increased when the antenna is attached with the LHM structure. The bandwidth has increased to 7% compared with the bandwidth without LHM structure. Figure 11 shows the measurement of radiation pattern for the patch antenna with and without LHM. From this radiation pattern, it shows that the gain of this antenna has been increased up to 4 dBi. The results correlate well between simulation and measurement.

In addition, the received power of the microstrip antenna with and without the LHM are also measured and shown in Figure 12. From those figures, it is obvious that the maximum power received by the antenna with LHM has increased dramatically about 4 dB. The comparison between the measurement results for antenna with and without LHM is shown in Table 3. Impressive result has been observed with a better return loss and maximum receive power as well as an increment in bandwidth of the designed microstrip patch antenna. This is due to the focussing effect of LHM structure.

3. CONCLUSIONS

In conclusion, a simulation, fabrication, and measurement are conducted for microstrip patch antenna incorporated with LHM. The findings show that there is an improvement in the antenna characteristics in term of bandwidth, gain, and directivity. The gain of the microstrip antenna with LHM is increased by 4 dB from simulation and measurement. Therefore, by using the

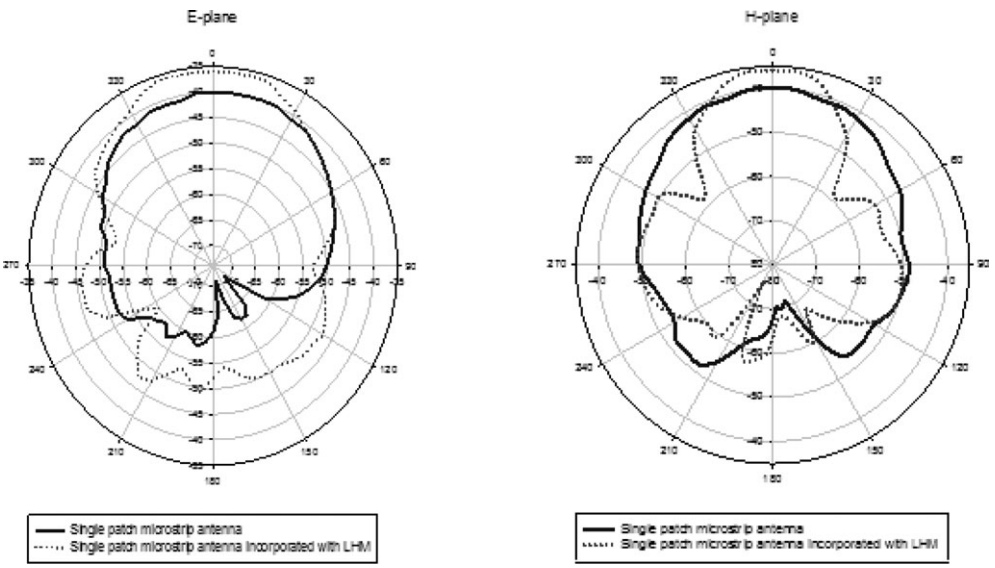

Figure 11 Measured radiation pattern at 5.8 GHz with and without LHM

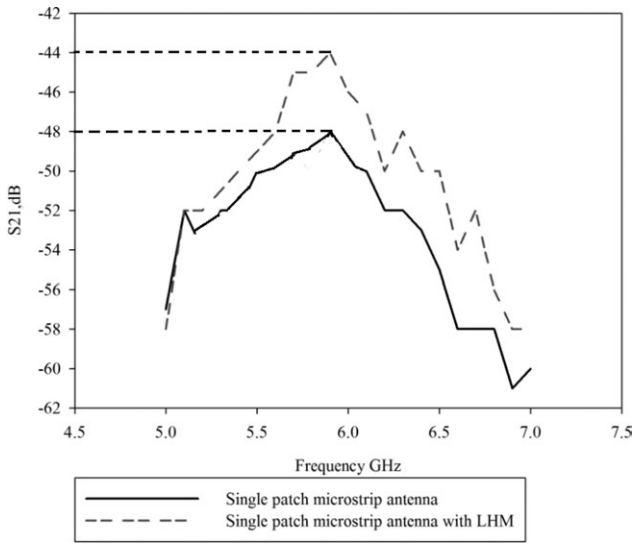

Figure 12 Measurement of received power for the microstrip antenna with and without LHM

TABLE 3 Comparison of Measurement Result

	Parameters at 6 GHz	Without LHM	With LHM
1	Return loss (S_{11})	−18.4 dB	−25.8 dB
2	Max power received	−48 dBm	−44 dBm
3	Bandwidth	4.3% (5.91–6.17 GHz)	7.4% (5.76–6.20 GHz)

LHM leads to a gain enhancement in the antenna performance. Moreover, the return loss (S_{11}) is improved by 15.71 dB with a bandwidth increased to 7% by incorporating the LHM structure. In summary, the LHM is recommended to be used in the modern antenna design for gain enhancement.

REFERENCES

1. V.G. Veselago, The electrodynamics of substances with simultaniously negative values of permittivity and permeability, Sov Phys Usp 10 (1968), 509.
2. Z. Wu, J. Zhu, M. Jia, H. Lu, and B. Zeng, A double layer metamaterial with negative refractive index originating from chiral configuration, Microwave Opt Technol Lett 53 (2011), 163–166.
3. C. Sabah, Multiband planar metamaterials, Microwave Opt Technol Lett 53 (2011), 2255–2258.
4. H.A Majid and M.K.A. Rahim, Parametric studies on left handed metamaterial consist of modified split ring resonator and capacitance loaded strip, Appl Phys A: Mater Proc 103 (2011) 607–610.
5. R.R. Ziolkowski, Double negative metamaterial design, experiment and applications, IEEE Trans Microwave Theory Tech 51 (2003).
6. J.B. Pendry, A.J. Holden, W.J. Stewart, and I. Youngs, Extremely low frequency plasmons in metallic mesostructures, Phys Rev Lett 76 (1996) 4773–4776.
7. J.B. Pendry, A.J. Holden, D.J. Robbins, and W.J. Stewart, Magnetism from conductors and enhanced nonlinear phenomena, IEEE Trans Microwave Theory Tech 47 (1999) 2075–2084.
8. D.R. Smith, W.J. Padilla, D.C. Vier, S.C. Nemat-Nasser, and S. Schultz, Loop-wire medium for investigating plasmons at microwave frequency, Phys Rev Lett 84 (2000) 4184.
9. M. Palandoken, A. Grede, H. Henke, Broadband microstrip antenna with left-handed metamaterials, IEEE Trans Antennas Propag 57 (2009), 331–338.
10. S.N. Burokur, M. Latrach, and S. Toutain, Theoretical investigation of a circular patch antenna in the presence of left-handed mematerial, IEEE Antennas Wirel Propag Lett 4 (2005).
11. Y. Lee and Y. Hao, Characterization of microstrip patch antennas on metamaterial substrates loaded with complementary split-ring resonators, Microwave Opt Technol Lett 50 (2011) 163–166.
12. T. Liu, X.-Y. Cao, J. Gao, Q. Yang, and W.-Q. Li, Design of miniaturized broadband and high gain metamaterial patch antenna, Microwave Opt Technol Lett 53 (2011) 2858–2861.
13. T.J. Cui, D.R. Smith, and R. Liu, Metamaterials theory, design, and applications, Springer, 2009.

BROADBAND BANDPASS FILTER USING OPEN COMPLEMENTARY SPLIT RING RESONATOR BASED ON METAMATERIAL UNIT-CELL CONCEPT

Kambiz Afrooz,[1] Abdolali Abdipour,[1] and Ferran Martín[2]
[1] Microwave/Millimeter-Wave and Wireless Communication Research Laboratory, Department of Electrical Engineering, Amirkabir University of Technology, Tehran, Iran; Corresponding author: kambaiz.afrooz@aut.ac.ir
[2] GEMMA/CIMITEC, Departament d'Enginyeria Electrònica, Universitat Autònoma de Barcelona, Bellaterra 08193, Barcelona, Spain

Received 7 March 2012

ABSTRACT: *In this article, a compact, wideband, and sharp rejection response bandpass filter based on metamaterial unit-cell concept is proposed. A series LC resonator using an interdigital capacitor and two meanders is designed, and an open complementary split ring resonator is used to realize the parallel LC resonator. Due to parasitic elements, achieving a pure series LC resonator has some difficulty. However, these parasitic elements can add two resonances more than conventional filters based on the metamaterial unit-cell. A design procedure based on a simple equivalent circuit is introduced. A compact bandpass filter at 1.475 GHz, with 94% fractional bandwidth, and an attenuation slope with 85.98 and 35.628 dB/GHz in the lower and upper transition bands, respectively, is designed and fabricated. The measured results are in good agreement with the full-wave electromagnetic simulations inferred by means of Agilent Momentum. The filter has very small size, that is, $0.341\lambda_g \times 0.1033\lambda_g$, where λ_g is the guided wavelength at the filter central frequency.* © 2012 Wiley Periodicals, Inc. Microwave Opt Technol Lett 54:2832–2835, 2012; View this article online at wileyonlinelibrary.com. DOI 10.1002/mop.27185

Key words: *bandpass filter; metamaterial; open complementary split ring resonator; interdigital capacitor; meander lines*

1. INTRODUCTION

Bandpass filters play an important role in communication systems to reject unwanted signals and to allow signal propagation in the desired pass bands. Wideband wireless communication systems are rapidly growing. Thus, wideband, compact, and highly selective bandpass filters are necessary components in wireless circuits [1]. Artificial metamaterial transmission lines have been applied to the design of microwave devices, such as power divider, couplers, phase shifters, and bandpass filters [2–5]. Bandpass filters based on metamaterial transmission lines have been investigated in microstrip, coplanar waveguide (CPW), and monolithic microwave integrated circuit technologies [5–8]. The canonical circuit models of the metamaterial unit-cell are shown in Figure 1. These circuit models are the T- and π-circuits, where the shunt branch is a parallel resonant tank, and the series branch is a series LC resonator. A balanced metamaterial unit-cell, that is, with identical series and shunt